

Do we understand the single-spin asymmetry for π^0 inclusive production in pp collisions?

Claude Bourrely and Jacques Soffer

Centre de Physique Théorique¹, CNRS-Luminy,
Case 907, F-13288 Marseille Cedex 9 - France

Abstract

The cross section data for π^0 inclusive production in pp collisions is considered in a rather broad kinematic region in energy \sqrt{s} , Feynman variable x_F and transverse momentum p_T . The analysis of these data is done in the perturbative QCD framework at the next-to-leading order. We find that they cannot be correctly described in the entire kinematic domain and this leads us to conclude that the single-spin asymmetry, A_N for this process, observed several years ago at FNAL by the experiment E704 and the recent result obtained at BNL-RHIC by STAR, are two different phenomena.

PACS numbers: 12.38.Bx, 13.85.Ni, 13.88.+e

CPT-2003/P.4581

¹Unité propre de Recherche 7061

High-energy single-spin asymmetries (SSA), usually denoted by A_N , in pion inclusive production $pp^\uparrow \rightarrow \pi X$, have been observed for the first time more than ten years ago, by the Fermilab E704 experiment [1, 2] at $p_{lab} = 200\text{GeV}/c$ ($\sqrt{s} = 19.4\text{GeV}$), in the beam fragmentation region. For clarity, we recall that A_N is defined as

$$A_N = \frac{d\sigma(\uparrow) - d\sigma(\downarrow)}{d\sigma(\uparrow) + d\sigma(\downarrow)}, \quad (1)$$

where $d\sigma(\uparrow), (d\sigma(\downarrow))$ is the π production cross section with one proton beam transversely polarized in the *up* (*down*) direction, with respect to the normal to the scattering plane. A striking dependence of A_N in Feynman variable x_F was observed, as shown in Fig. 1, for the neutral pion case, $pp^\uparrow \rightarrow \pi^0 X$. Very recently, the STAR Collaboration [3] at BNL-RHIC has released new data for the same SSA at $\sqrt{s} = 200\text{GeV}$, also depicted in Fig. 1. It is remarkable that these two sets of data cover approximately the same x_F range and, assuming that they have the same dynamical origin, it might be tempting to conclude that this SSA is energy independent, to a first approximation.

On the theoretical side, according to naive parton model arguments one expects $A_N = 0$, but several possible mechanisms have been proposed recently to generate a non-zero A_N . They are based on the introduction of a transverse momentum (k_T) dependence of either the distribution functions, for the Sivers effect [4] or of the fragmentation function, for the Collins effect [5]. These leading-twist QCD mechanisms have been used for a phenomenological study of this SSA [6] and higher-twist effects have been also considered [7, 8, 9]. However a simultaneous description of A_N and the unpolarized cross section has been ignored in all these works, a relevant point which has been already emphasized [10] and which will be crucial in the remaining of this paper.

Our starting point is the analysis of the cross section data in a broad kinematic region in the framework of perturbative QCD (pQCD), at next-to-leading order (NLO). It is a common belief that it should be best working in the central region, namely, for a π^0 produced near 90° , in the center-of-mass system, although some authors have argued that the phenomenological inclusion of intrinsic k_T effects leads to a better agreement between theory and data [11]. The inclusive invariant cross section for the reaction $pp \rightarrow \pi^0 X$ reads

$$E_\pi d\sigma/d^3p_\pi = \sum_{abc} \int dx_a dx_b f_{a/p}(x_a, Q^2, \mu_F) \times \\ f_{b/p}(x_b, Q^2, \mu_F) \frac{D_{\pi^0/c}(z_c, Q^2, \mu'_F)}{\pi z_c} d\hat{\sigma}/d\hat{t}(ab \rightarrow cX) , \quad (2)$$

where the sum is over all the contributing partonic channels $ab \rightarrow cX$ and $d\hat{\sigma}/d\hat{t}$ is the associated partonic cross section. In our calculations the parton distribution functions (PDF) $f_{a/p}, f_{b/p}$ are the BBS set constructed in Ref. [12] and $D_{\pi^0/c}$ is the pion fragmentation function BKK of Ref. [13]². μ_F and μ'_F denote two factorization scales and there is also a renormalization scale μ_R , associated to the running strong coupling constant α_s . Our calculations are done up to the NLO corrections, using the numerical code INCNLL of Ref. [15], with $\mu_F = \mu'_F = \mu_R = \mu$.

First we look at the cross section data at 90° for various energies, including data from ISR, Fermilab and BNL-RHIC, between $\sqrt{s} = 19.4\text{GeV}$ and 200GeV , as a function of p_T and the comparison with our calculations are displayed in Fig. 2. As it is well known, the agreement between theory and experiment depends on the choice of μ and this was extensively discussed, for example in Ref. [22]. For comparison we show the results for two scales $\mu = p_T$ and $\mu = p_T/2$ and we see that systematically the cross section for $\mu = p_T$ lies under that for $\mu = p_T/2$. In our case the best agreement occurs with $\mu = p_T$ for 200GeV and $\mu = p_T/2$ for 52.8GeV and below. We get a beautiful description of the PHENIX data but we have some disagreement at lower energies; we underestimate the data by a factor two on average and more for E706, in particular, at low p_T values. It is important to recall that the E704 Collaboration has also measured A_N in this kinematic region $\theta = 90^\circ$ and found $A_N = 0$ [16], up to $p_T = 4.5\text{GeV}/c$. The same trend has been observed recently by the PROZA-M experiment at $p_{lab} = 70\text{GeV}/c$ [17] and all these results are consistent with an earlier theoretical bound [18].

It is also crucial to note that in Fig. 1, whereas the STAR data points are at a fixed angle $\theta = 2.6^\circ$, this is not the case for the E704 data, for which $9^\circ < \theta < 67^\circ$, due to the simple relation $x_F = 2p_T/\sqrt{s}\tan\theta$ and the fact that $\langle p_T \rangle$ lies between 0.7 and 1 GeV/c. In this case, one can check that $A_N = 0$ for the three lowest x_F points which correspond to $\theta > 15^\circ$,

²We have checked that the KKP fragmentation functions of Ref. [14] give close numerical results

whereas A_N is not zero only for the four highest x_F points which correspond to $\theta < 15^\circ$.

This observation led us to examine the unpolarized cross sections away from $\theta = 90^\circ$, as a function of x_F , which combines the effects of p_T and θ . We have considered the ISR data [20] which have the largest angle coverage, they are shown in Figs. 3 and 4, with our numerical calculations. It is striking to observe that the NLO pQCD results give a smaller and smaller fraction of the measured cross section, when going to smaller and smaller scattering angles. At $\sqrt{s} = 23.3\text{GeV}$, which is very close to the E704 energy, for $\theta = 15^\circ$ the ratio Data/Theory can be one order of magnitude, even for $\mu = p_T/2$, which means that another mechanism is at work and dominates, very likely related to soft processes of some specific nature. At $\sqrt{s} = 52.8\text{GeV}$, we get a perfect description of the $\theta = 53^\circ$ data, for $\mu = p_T/2$, but again the relative size of the soft contributions increases in the forward direction, where the disagreement between data and pQCD gets larger. The failure of the NLO pQCD to reproduce the ISR small angle data is certainly not due to the breakdown of the convergence of the pQCD series in this region. Indeed the "K factor", defined as usual as $d\sigma_{NLO}/d\sigma_{LO}$, where LO stands for leading-order, is larger for small angles. We have also observed that there is a considerable reduction of the scale dependence, going from LO to NLO which shows an improvement in the perturbative stability. Therefore next-to-next-to-leading or higher pQCD corrections are not expected to account for a factor ten or so in the ratio Data/Theory.

Finally, we show in Fig. 5, the NLO pQCD calculations near the forward direction at $\sqrt{s} = 200\text{GeV}$ and one notices that at this energy, the $\theta = 2.6^\circ$ STAR data is very well reproduced by the solid curve ($\mu = p_T$). For the sake of completeness we also give our prediction (dashed curve) at $\theta = 4.2^\circ$, compared to the preliminary data released recently by the STAR Collaboration [3]. Now let us go back to the SSA measured by E704 and STAR shown in Fig. 1. In both cases, the data lie near the forward direction, but in the case of E704 it cannot be attributed to a pure pQCD mechanism, because the measured unpolarized cross section can be one order of magnitude higher than the pQCD result (see Fig. 3). On the other hand, it is very likely to be so in the case of STAR which has measured the cross section in full agreement with pQCD. Therefore this analysis strongly suggests that the two sets of SSA data, we have considered here, are the manifestation of two different phenomena, in contrast with the implications from Refs. [6, 7, 23].

To conclude, if pQCD does not generate a SSA in the $\theta = 90^\circ$ region, as

shown by E704, we dare to predict that PHENIX should also find $A_N = 0$, a result, indeed perfectly consistent with the recent rigorous positivity bound [24], which implies $|A_N| \leq 1/2$. It will be very interesting to know what the data analysis will give, when completed in the near future ³.

Note added : After this paper was completed, L. Bland and A. Ogawa have compared PYTHIA calculations of the invariant cross section with STAR and ISR data and they confirm our conclusions.

Acknowledgments: We thank W. Vogelsang for checking our numerical results and a very useful discussion. We are also grateful to M. Begel, G. Bunce, L. Bland and N. Saito for interesting comments and suggestions.

³This has been confirmed by very recent preliminary data [25].

References

- [1] E704 Collaboration, D.L. Adams *et al.*, Phys. Lett. B **264**, 462 (1991)
- [2] E704 Collaboration, D.L. Adams *et al.*, Phys. Lett. B **261**, 201(1991)
- [3] STAR Collaboration, G. Rakness, contribution to the XI Int. Workshop on Deep Inelastic Scattering (DIS2003), 23-27 April 2003, St. Petersburg, Russia; S. Heppelmann, contribution to the Transversity Workshop, 6-7 October 2003, IASA, Athens, Greece; J.Adams *et al.*, arXiv:hep-ex/0310058
- [4] D. Sivers, Phys. Rev. D **41**, 83 (1990); *ibid* D **43**, 261 (1991)
- [5] J.C. Collins, Nucl. Phys. B **396**, 161 (1993)
- [6] M. Anselmino *et al.*, Phys. Lett. B **442**, 470 (1998); Phys. Rev. D **60**, 054027 (1999)
- [7] J. Qui and G. Sterman, Phys. Rev. D **59**, 014004 (1999)
- [8] K. Kanazawa and Y. Koike, Phys. Lett. B **478**, 121 (2000); *ibid* B **490**, 99 (2000)
- [9] A.V. Efremov, V.M. Korotkiyan and O.V. Teryaev, Phys. Lett. B **348**, 577 (1995)
- [10] J. Soffer, A.I.P. Conference Proceedings **675**, 225 A.I.P. (2003)
- [11] E706 Collaboration, L. Apanasevich *et al.*, Phys. Rev. D **68**, 052001 (2003) and references therein
- [12] C. Bourrely, F. Buccella and J. Soffer, Eur. Phys. J., C **23**, 487 (2002). For a practical use of these PDF, see www.cpt.univ-mrs.fr/~bourrely/research/bbs-dir/bbs.html
- [13] J. Binnewies, B.A. Kniehl and G. Kramer Z. Phys. C **65**, 471 (1995); Phys. Rev. D **52**, 4947 (1995)
- [14] B.A. Kniehl, G. Kramer and B. Pötter, Nucl. Phys. B **582**, 514 (2000); *ibid* B **597**, 337 (2001)
- [15] F. Aversa *et al.* Nucl. Phys. B **327**, 105 (1989)

- [16] E704 Collaboration, D.L. Adams *et al.*, Phys. Rev. D **53**, 4747 (1996)
- [17] V. V. Mochalov *et al.*, arXiv:hep-ex/0312009
- [18] C. Bourrely and J. Soffer, Phys. Lett. B **71**, 330 (1977)
- [19] PHENIX Collaboration, S.S. Adler *et al.*, hep-ex/0304038
- [20] D. Lloyd Owen *et al.*, Phys. Rev. Lett. **45**, 89 (1980)
- [21] G. Donaldson *et al.*, Phys. Lett. B **73**, 375 (1978)
- [22] P. Aurenche *et al.*, Eur. Phys. J. C **13**, 347 (2000)
- [23] Y. Koike, A.I.P. Conference Proceedings **675**, 449 A.I.P. (2003)
- [24] J. Soffer, Phys. Rev. Lett. **91**, 092005 (2003)
- [25] C. Aidala, PHENIX Collaboration, Contribution to DIS2004, XII Int. Workshop on Deep Inelastic Scattering, 14 - 18 April 2004, Strbské Pleso, High Tatras, Slovakia

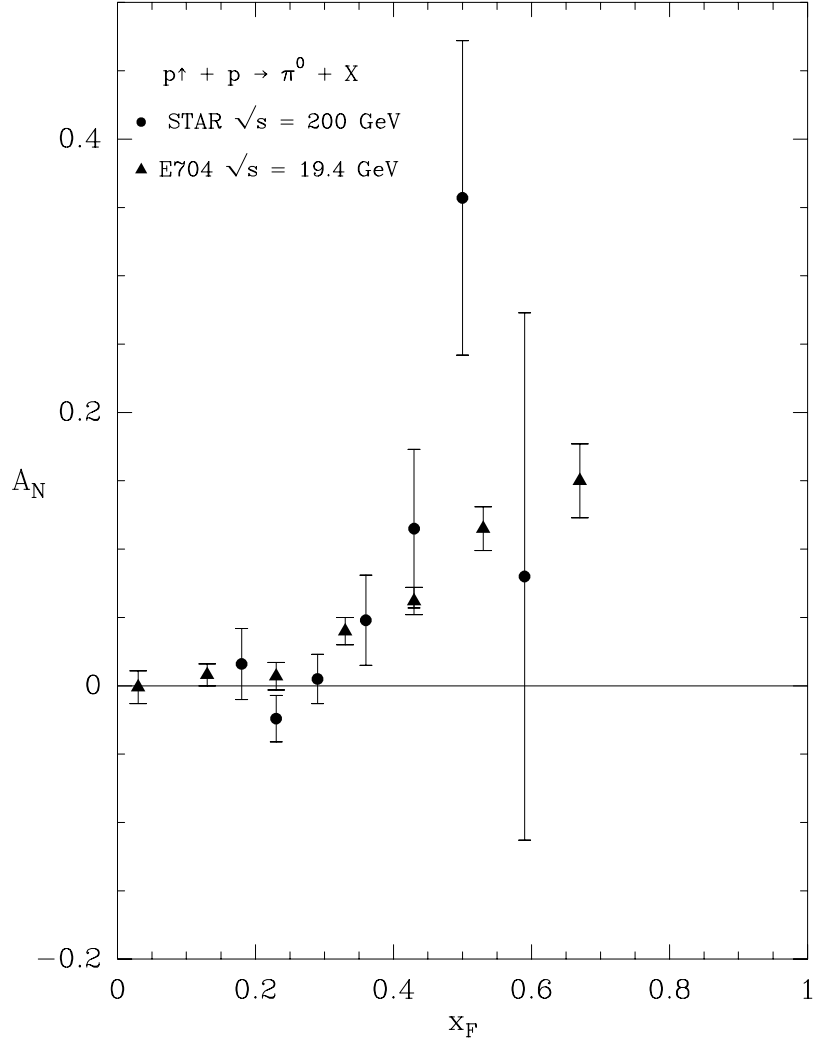


Figure 1: The single-spin asymmetry A_N as a function of x_F , at two different energies. The data are from Refs. [2, 3].

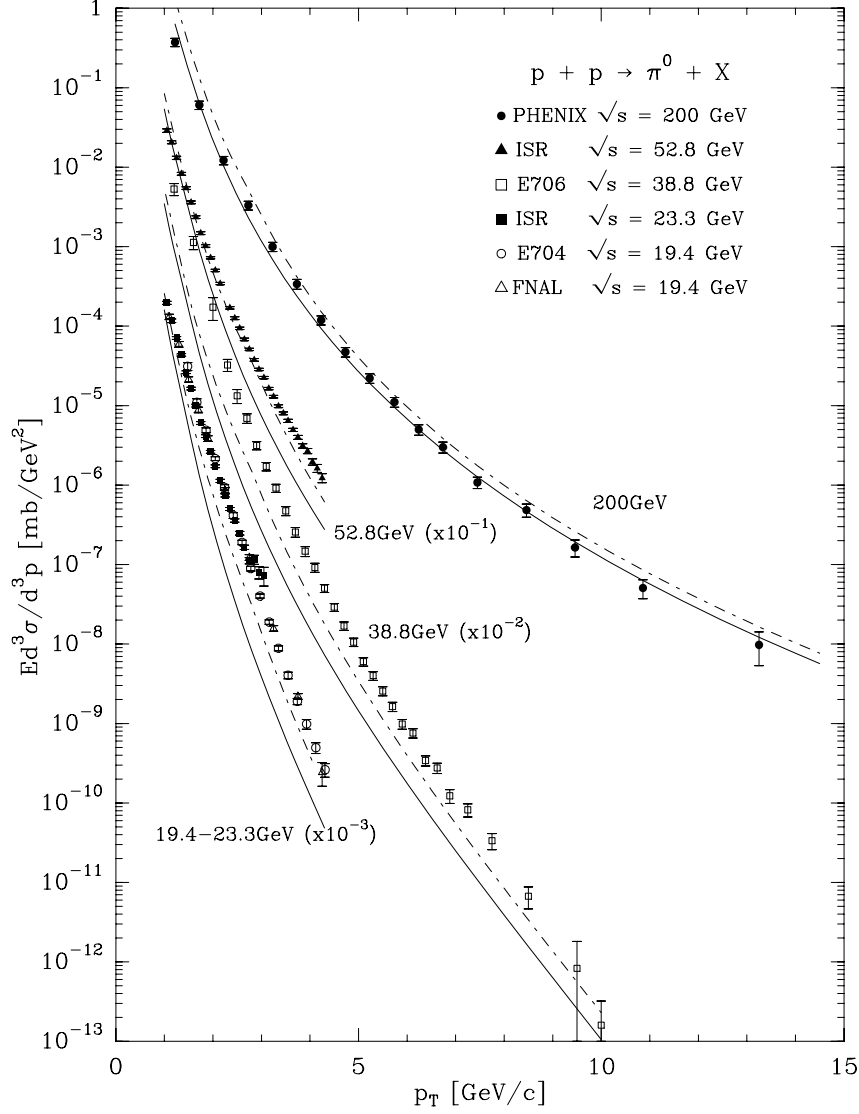


Figure 2: $Ed^3\sigma/d^3p$ at 90° and various energies, as a function of p_T . Data are from Refs. [11, 16, 19, 20, 21] and the curves are the corresponding NLO pQCD calculations with $\mu = p_T$ (solid lines) and $\mu = p_T/2$ (dotted- dashed lines).

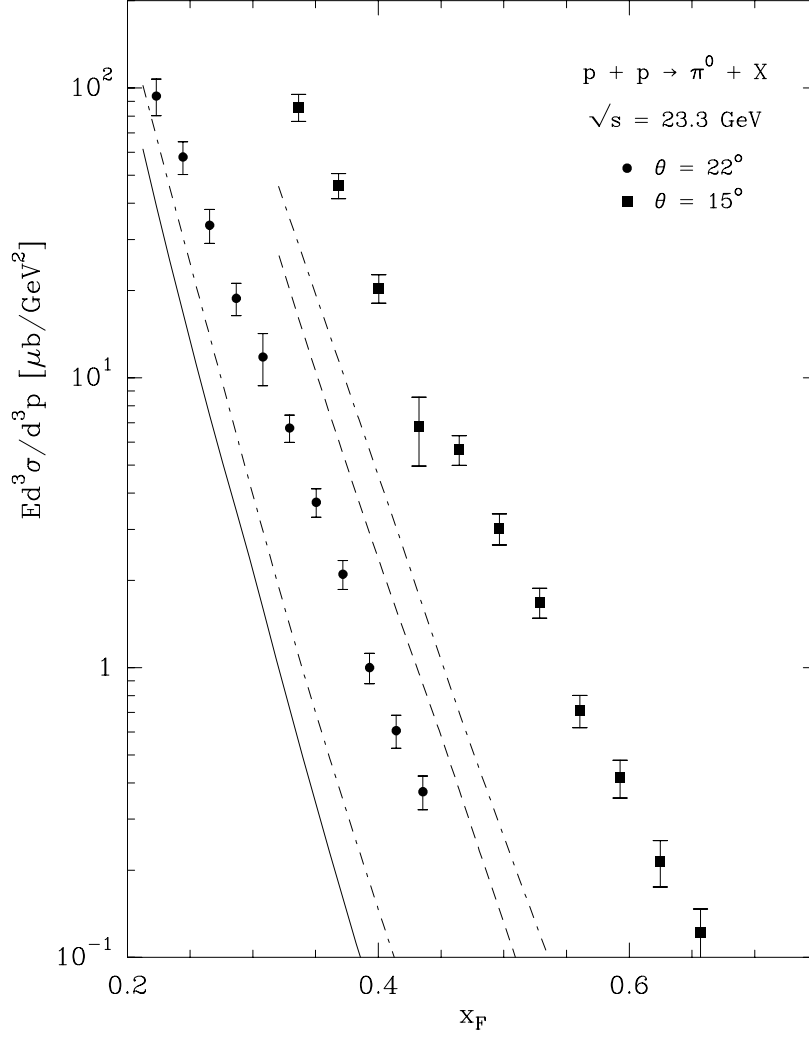


Figure 3: $E d^3 \sigma / d^3 p$ at $\sqrt{s} = 23.3 \text{ GeV}$, as a function of x_F for two different scattering angles. The data are from Ref. [20] and the curves, solid $\theta = 22^\circ$ and dashed $\theta = 15^\circ$, are the corresponding NLO pQCD calculations with $\mu = p_T$. The dotted-dashed curves are for $\mu = p_T/2$.

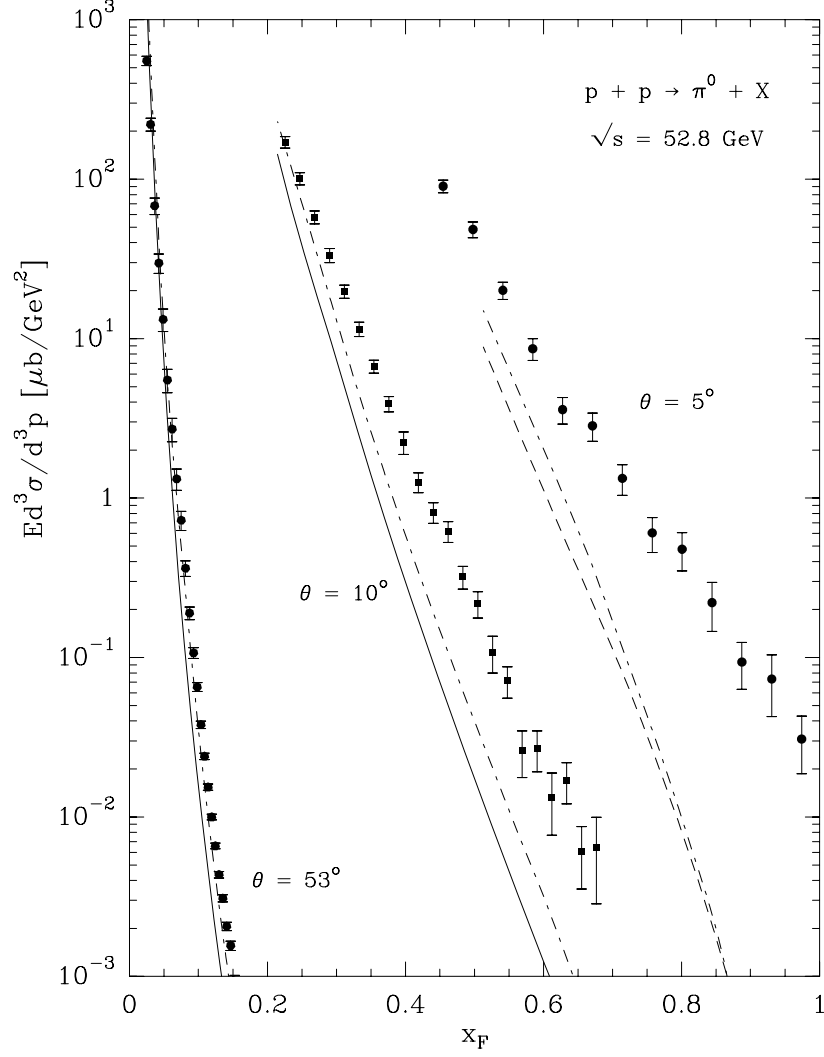


Figure 4: $Ed^3\sigma/d^3p$ at $\sqrt{s} = 52.8\text{GeV}$, as a function of x_F for three different scattering angles. The data are from Ref. [20] and the curves are the corresponding NLO pQCD calculations with $\mu = p_T$. The dotted-dashed curves are for $\mu = p_T/2$.

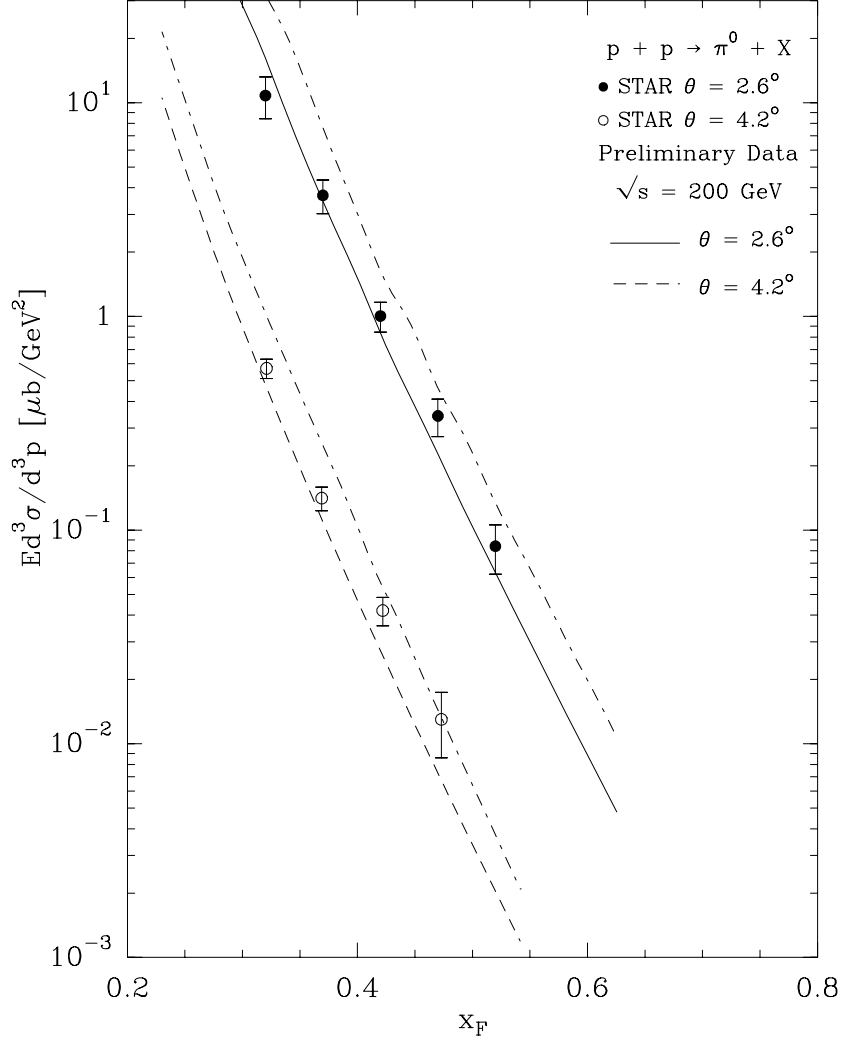


Figure 5: $Ed^3\sigma/d^3p$ at $\sqrt{s} = 200\text{GeV}$, as a function of x_F . The solid and dashed curves are the NLO pQCD calculations, with $\mu = p_T$, at two different angles and the data points are from Ref. [3]. The dotted-dashed curves are for $\mu = p_T/2$.